

Effects of Cl on the reduction of supported PdO in ethanol/water solvent mixtures

John B. Brazier, Mark A. Newton, Elena M. Barreiro, Stephen Parry, Luis A. Adrio, Christopher J. Mulligan, Klaus Hellgardt, King Kuok (Mimi) Hii, Paul B. J. Thompson, Rachel Nichols & Bao N. Nguyen

To cite this article: John B. Brazier, Mark A. Newton, Elena M. Barreiro, Stephen Parry, Luis A. Adrio, Christopher J. Mulligan, Klaus Hellgardt, King Kuok (Mimi) Hii, Paul B. J. Thompson, Rachel Nichols & Bao N. Nguyen (2017) Effects of Cl on the reduction of supported PdO in ethanol/water solvent mixtures, *Catalysis, Structure & Reactivity*, 3:1-2, 54-62, DOI: [10.1080/2055074X.2016.1267296](https://doi.org/10.1080/2055074X.2016.1267296)

To link to this article: <http://dx.doi.org/10.1080/2055074X.2016.1267296>



© 2017 The Author(s). Published by Informa UK Limited, trading as Taylor & Francis Group



Published online: 21 Feb 2017.



Submit your article to this journal [↗](#)



Article views: 141



View related articles [↗](#)



View Crossmark data [↗](#)

Effects of Cl on the reduction of supported PdO in ethanol/water solvent mixtures

John B. Brazier^a , Mark A. Newton^b, Elena M. Barreiro^a, Stephen Parry^c , Luis A. Adrio^a, Christopher J. Mulligan^a , Klaus Hellgardt^d , King Kuok (Mimi) Hii^a , Paul B. J. Thompson^{e,f}, Rachel Nichols^g and Bao N. Nguyen^g

^aDepartment of Chemistry, Imperial College London, London, UK; ^bDepartment of Physics, University of Warwick, Coventry, UK; ^cDiamond Light Source, Didcot, UK; ^dDepartment of Chemical Engineering, Imperial College London, London, UK; ^eDepartment of Physics, University of Liverpool, Liverpool, UK; ^fXMaS CRG, European Synchrotron Radiation Facility, Cedex, France; ^gSchool of Chemistry, University of Leeds, Leeds, UK

ABSTRACT

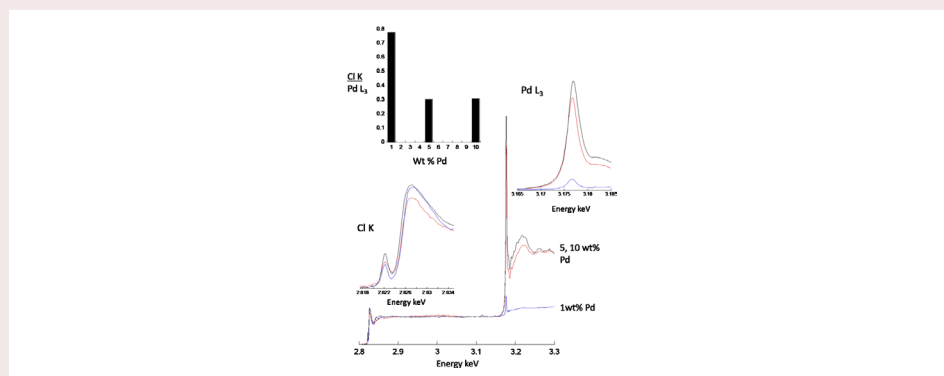
The reduction of γ -Al₂O₃-supported PdO in flowing aqueous ethanol was investigated. Quick EXAFS (QEXAFS) performed at the Pd K-edge reveals that the presence of Cl can have a profound effect on the reduction process. At low loadings of Pd (1 wt-%), the size dependency of the process is inverted, compared to Cl-free samples. The extent of reduction was found to be dependent on loading/particles size. It is shown, using *in situ* QEXAFS at the Cl K- and Pd L₃-edges, that residual Cl is not removed by the flowing solvent mixture, even at an elevated temperature of 350 K. The origins of these behaviours are discussed in terms of the differing effects that Cl may have when bonded to oxidic or reduced metal centres and the results were compared to earlier observations made on the effects of Cl on commercial polyurea encapsulated Pd ENCATTM NP 30 catalysts.

ARTICLE HISTORY

Received 12 October 2016
Accepted 25 November 2016

KEYWORDS

Quick EXAFS; chlorine; Palladium; green solvents; reduction; hydride formation; operando measurement



Introduction

Solvents are widely employed by the fine chemicals and pharmaceutical industries in their manufacturing processes to solubilise reactants during the reaction, as well as downstream processes for product separation and purification. As a result, the use of solvents has been identified as the biggest contributor to the economic and environmental costs of a chemical manufacturing process. In order to minimise these impacts, there are a number of solvent selection guides published in recent years, which aim to define what is a “green” solvent [1–4], assessed by its safety, health and environmental criteria.

Palladium is one of the most versatile elements used to catalyse a broad range of reactions that are particularly relevant to the fine chemicals and pharmaceutical industries, from the hydrogenation of unsaturated bonds, to C–C and C–X bond forming reactions [5]. In recent years, there has been particular interest in translating the myriad of Pd-catalysed reactions into continuous flow processes, which will require the use of a heterogeneous or immobilised form of the catalyst. In these cases, leaching of Pd into the mobile phase, either as molecular species or as colloids, is a significant problem [6–9], as it directly affects catalyst longevity, recovery, and purification of the product, which have thus far restricted

CONTACT Mark A. Newton  M.Newton.2@warwick.ac.uk; King Kuok (Mimi) Hii  mimi.hii@imperial.ac.uk

© 2017 The Author(s). Published by Informa UK Limited, trading as Taylor & Francis Group.

This is an Open Access article distributed under the terms of the Creative Commons Attribution License (<http://creativecommons.org/licenses/by/4.0/>), which permits unrestricted use, distribution, and reproduction in any medium, provided the original work is properly cited.

wider application of supported Pd catalysts within the pharmaceutical industry.

To address this problem, we have initiated a programme study, using operando Quick Pd K-edge EXAFS (QEXAFS) to investigate the effect of a flowing ethanol-water mixture on a number of Pd catalysts, containing different phases and size distributions of Pd nanoparticles supported upon different dispersant materials [10–12]. Concurrently, we have also investigated the behaviour of polymer encapsulated (ENCAT™) Pd catalysts under the same conditions [13]. Through this work we have shown that supported PdO shows strong particle size dependence towards reduction in ethanol-water mixtures: small PdO particles (< ca. 3 nm) show a pronounced resistance to reduction compared to bigger particles (>4 nm), which are relatively easily reduced by the solvent flow. Pd that exists in very highly dispersed metallic states can react extremely readily with the flowing ethanol-water mixture. These forms of Pd readily agglomerate, under relatively mild reaction conditions, to yield much larger and less dispersed Pd particles [12]; a process that polymer encapsulation can curtail [13]. Lastly, these behaviours appear to be relatively independent of the support materials thus far investigated, and all the reduced Pd nanoparticles formed are significantly contaminated by interstitial hydrogen. This last observation is of particular importance, given that the formation of PdH_x phases can have significant effect on the surface reactivity [14–17].

Cl is an important impurity that can be present in either the metallic particle, or in the support material, particularly if chloride precursors were employed in their synthesis. In many catalyst systems, the presence of the halide anion is known to affect various aspects of the generation and subsequent behaviour of these materials [18–22]. In this paper we will apply the same approach, combining Quick Pd K-edge EXAFS (QEXAFS) with Cl and Pd L₃ edge XANES, to examine the role of residual Cl in the reduction of Al₂O₃ supported Pd catalysts.

Experimental

Catalyst synthesis

Chlorinated Pd catalysts were prepared by wet impregnation, using PdCl₂ as a metal precursor, and γ-Al₂O₃ (Alfa Aesar; pellets pre-ground/sieved to between a 90 and 75 μm mesh fraction) as described previously [23,24], followed by drying in air at 373 K. The samples were then calcined in flowing air (1 K min⁻¹ ramp to 773 K and held at temperature for 4 h before cooling at 1 K min⁻¹). Once cooled the samples were then sieved again to a 75–90 μm mesh fraction before use. The equivalent Cl-free catalysts were similarly prepared by using Pd(NO₃)₂ solutions (15.05 wt-% Pd, Johnson Matthey PLC) as the metal precursor.

Operando spatio-temporal QEXAFS measurements at the Pd K edge

QEXAFS measurements were made at the core EXAFS beamline B18 [25,26] of the Diamond Light Source, using a Si (1 1 1) double crystal monochromator and ion chambers for detection of X-ray absorption, normalisation, and energy scale (Pd foil) calibration. The dimensions of the X-ray beam used to sample through the 4 mm i.e. sample bed were 0.5 mm (height) × 2 mm (width). Bi-directional QEXAFS was employed with a time per (uni-directional) spectrum (24–25.5 keV) of ca. 10–20 s. During experimentation QEXAFS spectra were sequentially collected along the catalyst bed at intervals of 0.5 mm, starting at the inlet and ending at the outlet. This process was then repeated throughout the remainder of the experiment. Data reduction was made using “Prestopronto” XAFS [27] software or PAXAS [28] prior to EXAFS analysis using EXCURV [29].

The continuous flow reactor and the overall experimental protocols followed in this study have been fully described elsewhere [10]. Briefly, the solvent used comprised of a 50:50 v/v mixture of H₂O/EtOH. The solvent components were individually degassed using nitrogen gas bubbled through the liquids, followed by sonication after mixing. The sample was packed into a quartz tube – to yield beds of ca. 5 mm in length – and secured on either side using γ-Al₂O₃ of a smaller particle size and then quartz sand. Once loaded in the reactor the sample was located and mapped in a dry state prior to the solvent being pumped through at 0.1 mL min⁻¹ flow and the “wet” bed was mapped again. The sample was then heated at 1 K min⁻¹ under the flowing solvent to 350 K whereupon it was held at this temperature for the remainder of the experiment. Pd K-edge EXAFS maps of the bed were continually collected throughout with a single complete axial map of the bed being obtained every 5–7 min.

In situ Cl K and Pd L₃ edge spectroscopy

Cl K edge and Pd L₃ edge measurements were made at the XMaS beamline at the ESRF using a Si (1 1 1) double crystal monochromator and a Ketek Silicon fluorescence detector. A description of the overall setups and methodologies employed can be found in a previous publication [30]. In the measurements presented here acquisition times were typically 5–10 s/point through a 5 μm thick polyethylene window. Solvents were applied to the catalysts under the same conditions (flow rate and temperature ramp) used for the Pd K edge EXAFS measurements.

Results

Three Pd/γ-Al₂O₃ catalysts containing different weight loadings of the metal (1, 5 and 10 wt-%) were prepared from a chloride precursor. The Pd K-edge EXAFS

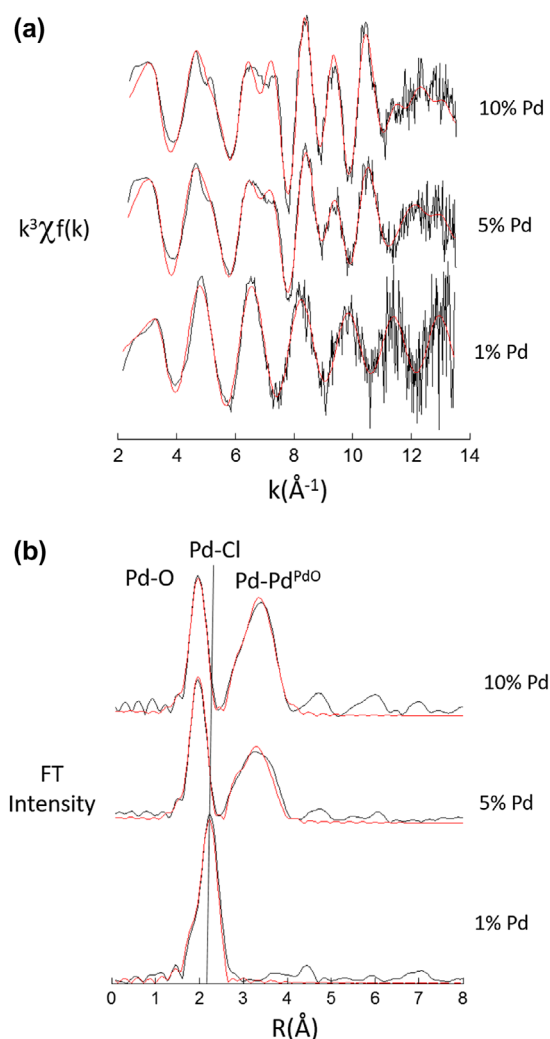


Figure 1. (a) k^3 -weighted Pd K-edge EXAFS and (b) the corresponding Fourier transforms for the three Pd/Al₂O₃ catalysts derived from PdCl₂ precursor. Measured as dried samples at RT. The red lines are fits to the data derived in Table 1.

spectra of the dried catalysts (mounted as a packed bed in the Stokes flow reactor) were recorded (Figure 1); the

structural and statistical parameters derived from analysis of the EXAFS spectra using EXCURV are presented in Table 1. Compared with the data acquired previously of the equivalent catalysts prepared from a Cl-free precursor [11], the 5 and 10 wt% Pd catalysts are found to comprise nanosize PdO without any reduced Pd(0) being present. In contrast, the 1 wt-% Pd/ γ -Al₂O₃ catalyst is very different. The distinctive O, Pd and Pd scattering shells characteristic of PdO found in the 1 wt-% catalyst prepared from a Cl-free precursor were absent; instead, the EXAFS spectrum is dominated by a scattering peak between 2.3 and 2.4 Å from the central Pd atom, which corresponds to a significant Pd–Cl interaction, indicating the presence of Cl that has been retained in the nanoparticle and bound to the Pd. Alongside this scattering shell, there is also an accompanying Pd–O scattering interaction. Hence, the chlorinated and calcined 1 wt-% Pd/ γ -Al₂O₃ catalyst appears to consist of supported Pd oxychloride, with an inferred stoichiometry of *ca.* PdCl₂O₂, rather than PdO.

The samples were then wetted by a flowing liquid stream of 50% v/v ethanol-water at ambient temperature. The corresponding EXAFS spectra (Figure 2) shows that the PdO species present in the 5 and 10 wt-% catalysts, remained essentially unchanged, as was expected based upon our previous observations of the behaviour of their Cl-free analogues [11]. For the 1 wt-% Pd/ γ -Al₂O₃, exposure to the flowing solvent at room temperature elicits significant change in the habit of the Pd. In this case, a decrease in the Pd–Cl scattering shell is accompanied by a growth of a significant Pd–O interaction and a reduction of Pd–Pd scattering; associated with the formation of a nascent metallic Pd phase (Table 1). The ease of this Pd sample marks a sharp contrast to its Cl-free analogue, which was resistant to reduction under the same conditions.

These studies were supplemented further by EXAFS data collected at the Cl K- and Pd L₃- edges, using

Table 1. Structural and statistical parameters arising from the analysis of k^3 -weighted Pd K-edge EXAFS for the three chlorinated Pd/ γ -Al₂O₃ catalysts in their dry and wet states.

% Pd	Shell	Dry					Wet					
		N^a	R^b (Å)	DW ^c ($2\sigma^2$)	E_f	$R\%$	N^a	R^b (Å)	DW ^c ($2\sigma^2$)	E_f	$R\%$	
10 wt-%	O	3.9	2.03	0.01	3.1	33.0	3.9	2.02	0.01	3.4	29.5	
	Pd	3.7	3.05	0.01								
	Pd	5.4	3.44	0.02								
5 wt-%	O	4.0	2.03	0.01	3.9	33.4	3.6	2.02	0.01	3.5	33.5	
	Pd	3.0	3.04	0.01								
	Pd	2.7	5.44	0.02								
1 wt-%	Cl	2.1	2.29	0.01	1.9	52.3	2.7	2.00	0.01	-1.7	66.0	
	O	1.6	2.01	0.01								
	Pd											1.5

^aCo-ordination number ($\pm 10\%$ of stated value);

^bdistance of the scattering atom from central atom ($\pm 1.5\%$ of stated value);

^cDebye-Waller factor = $2\sigma^2$, where σ is the root mean square inter-nuclear separation (Å). E_f = the edge position relative to the vacuum zero (Fermi energy, eV).

$R\% = \left(\int \frac{| \chi^T - \chi^E | k^3 dk}{| \chi^T | k^3 dk} \right) \times 100$ where χ^T and χ^E are the theoretical and experimental EXAFS and k is the photoelectron wave vector. Other parameters: AFAC, related to the proportion of electrons performing an EXAFS type scatter on absorption, is 1. The fitting range used was: $k = 2.5\text{--}13.5 \text{ \AA}^{-1}$.

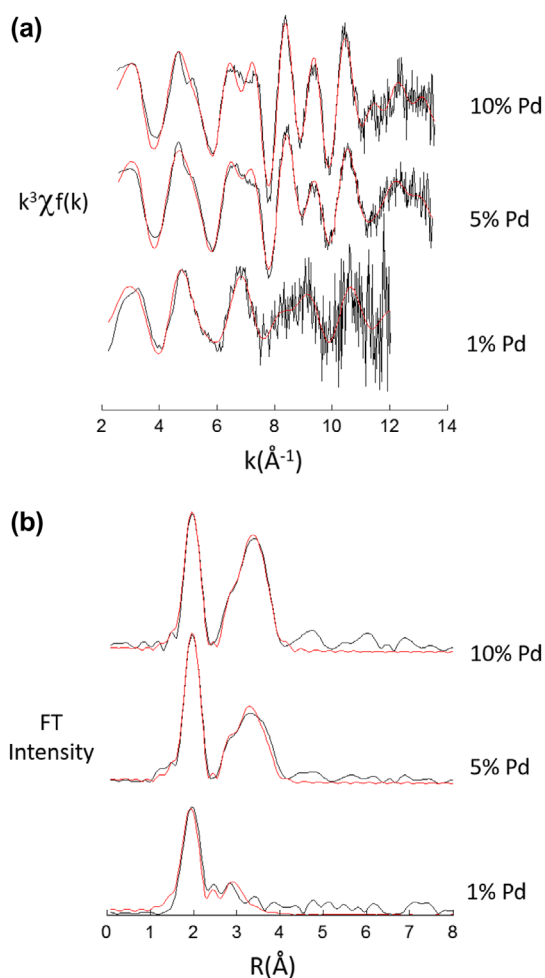


Figure 2. (a) k^3 -weighted Pd K-edge EXAFS and (b) the corresponding Fourier transforms for three (1, 5 and 10 wt-%) Pd/Al₂O₃ catalysts derived from PdCl₂, measure at ambient temperature under a flowing 50:50 ethanol/water. The red lines are fits to the data derived in Table 1.

methods we have recently developed at the XMaS beamline at the ESRF [30]. Figure 3 shows the results for the dry samples, which clearly indicated the amounts of Cl retained in these catalysts – relative to the Pd loading – is considerably higher in the 1 wt-% case compared to the 5 and 10 wt-% cases. The presence of a pre-edge feature in the Cl K-edge indicates that a significant fraction of the total level of Cl retained is bound directly to Pd in each of these catalysts. With reference to a PdCl₂ standard, and assuming that the normalised intensity of this pre-edge features is directly proportional to the fraction of Cl atoms directly bound to oxidised Pd (PdO), we estimate that between 22 and 33% of the total Cl present in these dry sample is attached to Pd; the remainder is assumed to be bonded to Al centres at the surface of the support: Cl bound in this configuration, or indeed to Pd⁰, does not show a pre-edge feature at the Cl K-edge [31–33].

Once the catalysts are subjected to the flowing solvent mixture, the Cl K-edge XANES showed a significant reduction in the relative intensity of the pre-edge feature (Figure 4), which implies a loss of Cl bonded to oxidised Pd centres, suggesting that some of this Cl

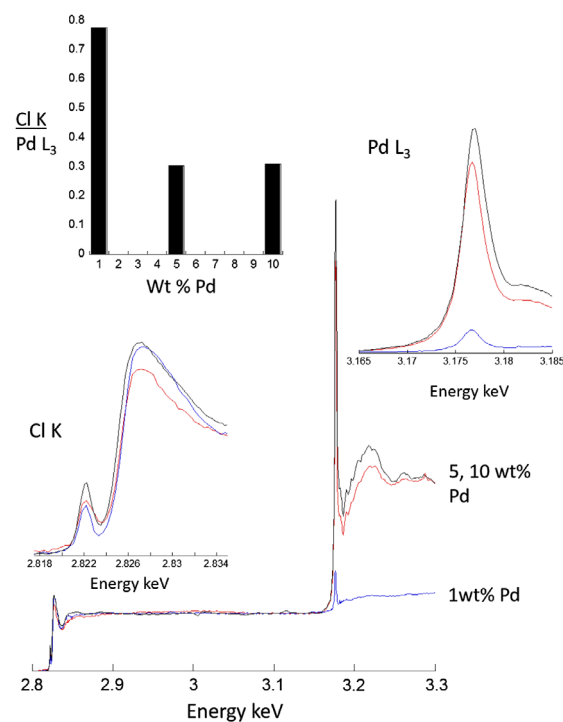


Figure 3. Normalised Cl K- and Pd L₃-edge XAS derived from the three chlorinated Pd/γ-Al₂O₃ catalysts. Insets: expansion of the Cl K edge and Pd L₃ edge XANES regions. The uppermost inset gives the raw Cl K/Pd L₃ edge jump ratios (relative to the Cl K edge) as a function of the loading of Pd in the sample.

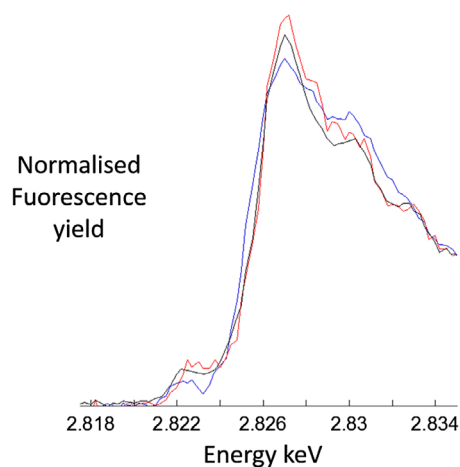


Figure 4. Cl K-edge XANES derived from the 1 wt-% (blue), 5 wt-% (red), and 10 wt-% (black) catalysts under a flowing ethanol/water mixture at room temperature.

is washed from the catalyst completely and lost to the mobile phase of solvents. However, it is also possible that the observed changes in X-ray absorption may be due to the solvent absorption of Cl K- and Pd L₃-fluorescence, and the effect is more pronounced for Cl fluorescence intensity (at lower energy) compared to the Pd L₃ X-rays. An equally plausible explanation is the displacement of some of the Cl from the Pd to Al sites on the support.

At this juncture, we may surmise that the first consequence of the wetting of all the samples with ethanol-water is to remove a proportion of the Cl directly

bonded to the Pd (in the 5 and 10 wt-% cases). Equally some Cl remains within the system and is not leached to the solvent flow at this temperature. By contrast we only have an indication that Cl–Pd bonding is lost in the 1 wt-% Pd case from the Pd K-edge EXAFS.

Having characterised the dry and wet samples at ambient temperature, each of the catalysts was subsequently heated under the solvent flow. At the same time, spatio-temporal mapping along the catalyst bed was undertaken using Pd K-edge QEXAFS to evaluate how the Pd within the systems would develop. Two structural parameters may be extracted from analysis of the EXAFS: the coordination of number of the PdPd scattering interaction, N_1^{PdPd} (Figure 5), which is characteristic of the development of an *fcc* Pd structure i.e. metallic Pd nanoparticles; and the bond distance (\AA) associated with the PdPd scattering interaction, R_1^{PdPd} (Figure 6), which is indicative of metallic Pd nanoparticles. In the case of Figure 5 the development of N_1^{PdPd} as a function of axial position in the bed and temperature is directly comparable to the previous study performed with non-chlorinated samples [11].

The results showed that the reduction of Pd in these systems is dependent upon the loading in both chlorinated and non-chlorinated cases. In the case of 10 wt-% Pd loadings, the evolution of an *fcc* nanoparticulate Pd phase is the same regardless of whether Cl is present. The only difference is the maximum values of N_1^{PdPd} achieved – *ca.* 7 versus *ca.* 9 for chlorinate and non-chlorinated samples, respectively. The chlorinated catalyst also shows a narrower range of N_1^{PdPd} values along the length of the bed. In contrast, the non-chlorinated catalysts persistently return very low (<4) values of N_1^{PdPd} at the reactor inlet.

The first of these observations might be indicative of the reduced Pd nanoparticles being somewhat smaller in the chlorinated case than they are in the Cl-free case. Reference to earlier studies of Benfield [34] and Jentys [35], this might indicate that the Pd particles created from the chlorinated sample might be, on average, 3–6 times smaller than those derived from the reduction of a non-chlorinated source, in terms of their average particle atomicity, i.e. the average number of Pd atoms they contain.

The 5 wt-% samples also show similar evolution in the Pd structure, in terms of N_1^{PdPd} . In this case, the onset temperature for reduction of the chlorinated sample is lowered slightly. Once again, lower values of N_1^{PdPd} is found at the inlet of the reactor, than in the remainder of the bed (towards the reactor outlet) though these differentials are not as great in the chlorinated case as they are in the Cl-free sample. For the 5 wt-% catalysts, the reduced samples appear to converge towards maximal values of N_1^{PdPd} (8–8.5), implying that they arrived at similar average particle sizes, at least within the experimental limits of EXAFS to make this determination [34].

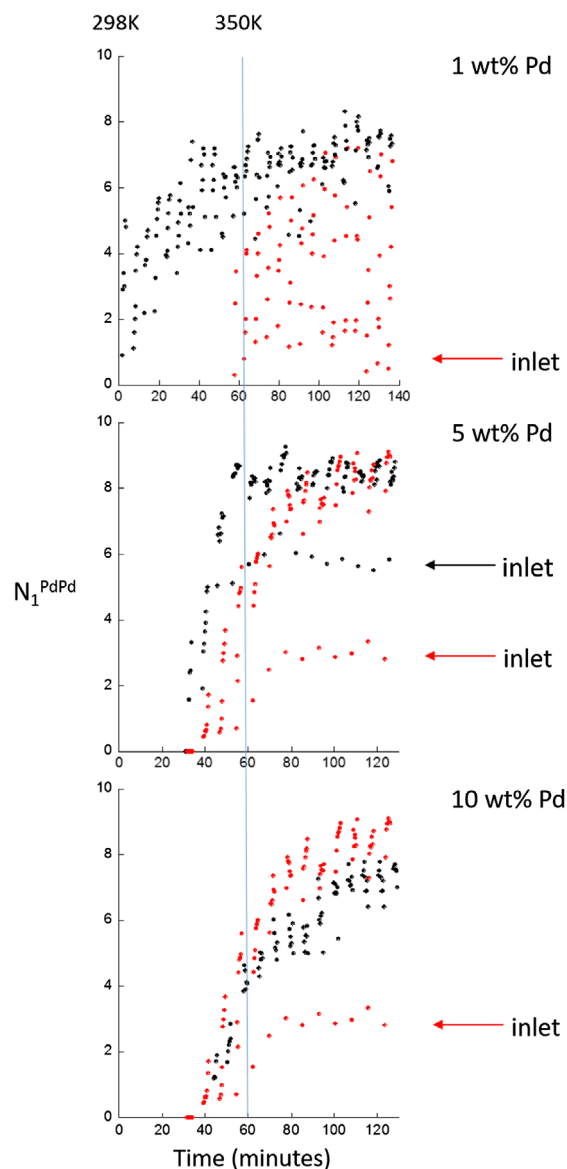


Figure 5. Evolution of the three Pd/ γ -Al₂O₃ catalysts derived from PdCl₂ (as indicated, black symbols) and the equivalent catalysts derived from Pd nitrate (red), heated at 1 k min⁻¹ under flowing ethanol/water to *ca.* 350 K: The coordination number of the first shell *fcc* Pd (N_1^{PdPd}) returned from the analysis of the spatio-temporally resolved QEXAFS. The vertical blue line indicates the point at which the samples reaches 350 K. Thereafter they are maintained isothermally. This graph contains the results obtained from all axial position within the catalyst bed and therefore also yield information regarding phase and particle size gradients that exist.

Last but not least, the 1 wt-% Pd/ γ -Al₂O₃ samples show the greatest difference in their behaviour, with the chlorinated sample undergoing reduction at room temperature, whereas the equivalent non-chlorinated system resists any reduction until 350 K and, even then, only reduces significantly at the very outlet of the catalyst bed, displaying a considerable axial variation in N_1^{PdPd} . As we have already seen the chlorinated 1 wt-% catalyst has a fundamentally different structure to the 1 wt-% non-chlorinated sample that appears to imbue it

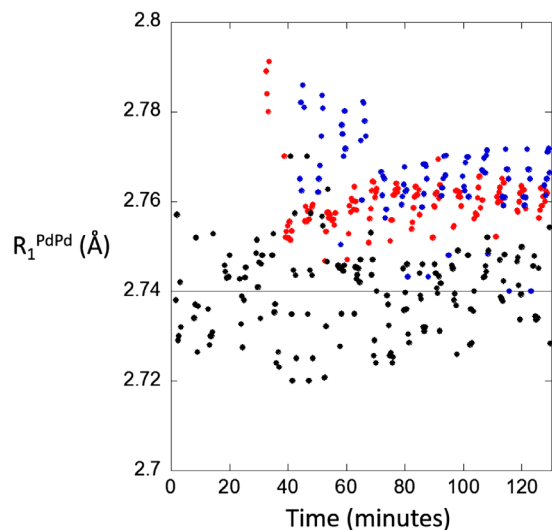


Figure 6. Variation of the PdPd bondlength, R_1^{PdPd} (Å), associated with the 1st shell *fcc* PdPd scattering interaction N_1^{PdPd} (Figure 5) derived from the three chlorinated Pd/ γ -Al₂O₃ catalysts, heated and maintained at 350 K under flowing ethanol/water. Black = 1 wt-%, red = 5 wt-%, and blue = 10 wt-% Pd. The horizontal black line is the average value of R_1^{PdPd} returned from analysis of the Pd foil measured in parallel with the sample.

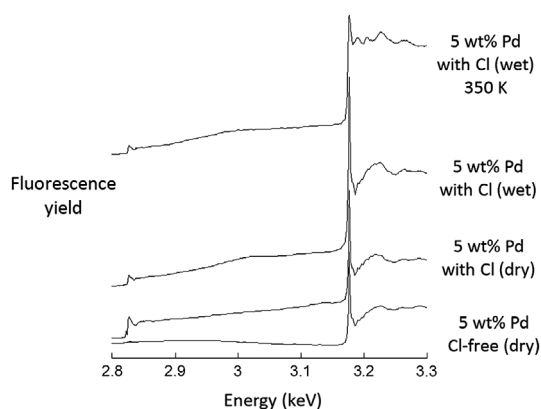


Figure 7. Evolution of a chlorinated 5 wt-% Pd/ γ -Al₂O₃ sample under flowing ethanol/water from the perspective of the Cl K- and Pd L₃-edges. The bottom spectrum is derived from an equivalent 5 wt-% Pd catalysts derived from a Cl free precursor measured in the absence of solvent.

with a much lower resistance to reduction by the solvent mixture.

The nature of the reduced Pd can be derived from the PdPd bondlength associated with the metallic nanoparticles as they are formed (Figure 6). For both 5 and 10 wt-% Pd/ γ -Al₂O₃ catalysts (red and blue data points), values of R_1^{PdPd} are significantly above that expected from a reference Pd foil. Even in the case of the 1 wt-% catalyst (black data point) the value of R_1^{PdPd} from the EXAFS is approximately equal to that obtained from the Pd foil (measured in tandem with the samples). Once again, we can conclude that the particles formed by reduction in the solvent mixture are significantly contaminated with interstitially adsorbed atomic hydrogen [10,11].

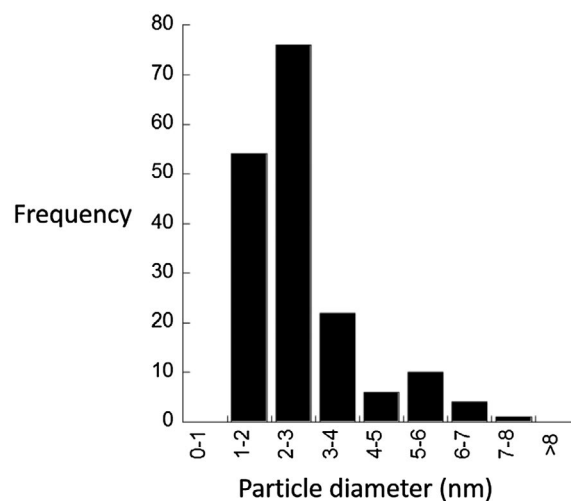
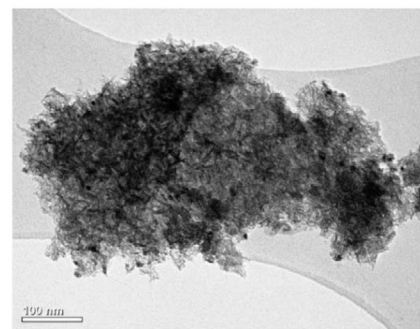


Figure 8. Transmission electron microscopy derived from the chlorinated 1 wt-% Pd/Al₂O₃ sample. (a) A representative micrograph; (b) particle size distribution derived from several micrographs.

Figure 7 shows the results obtained from the equivalent *in situ* experiment made at the Cl K- and Pd L₃-edges for the 5 wt-% Pd/ γ -Al₂O₃. Globally these spectra support the conclusions drawn from the Pd K-edge EXAFS spectra, insofar as the Pd phase is clearly reduced by the solvent at $T = 350$ K.

For comparison, the data was compared to an equivalent, Pd nitrate-derived system (bottom trace), measured in the absence of solvent to confirm that the Al₂O₃ used is, in fact, chlorine free, having previously found that certain other aluminas [30] contain considerable levels of chlorine that can interact with metals deposited. Beyond this, we may see that after having been wetted at room temperature, the residual chlorine that remains in the sample is not subsequently removed, or change significantly, through subsequent heating under the solvent flow. Once again, it is not possible to tell, at this juncture, where this persistent Cl actually resides in these catalysts, bound to the reduced Pd nanoparticles, or resides at acid sites on the γ -Al₂O₃.

In earlier work, we have shown that significant rearrangement of Pd can occur during sample preparation, which can potential lead to erroneous results [12]. In the present work, we have shown that the reduction of the chlorinated 1 wt-% Pd/ γ -Al₂O₃ catalyst can occur in a very facile manner under ambient conditions in an alcoholic

solvent. Indeed, the TEM image of the sample shows the presence of well-defined nanoparticles (Figure 8), which is significantly different from the EXAFS analysis performed of the dry sample using EXAFS (Figure 1 and Table 1). This serves to highlight the advantage of the spectroscopic method for structure determination across different sample environments.

Discussion

The amount of Cl retained in a Pd catalyst, prepared by the wet-impregnation method, is dependent upon the total loading of Pd on γ - Al_2O_3 . In 5 wt-% and 10 wt-% cases the native phase is largely nanoparticulate PdO, while at a lower Pd loading (1 wt-%), the Pd phase is present as an oxychloride of approximate stoichiometry PdCl_2O_2 .

In each of the dry catalysts, the presence of a pre-edge feature in the Cl K-edge XANES, shows that some 20–30% is found to be still bonded directly to the Pd. For the most part, however, under the flow of solvent, this Cl–Pd bonding is removed, even at room temperature, with the majority of the Cl most likely lost to the solvent flow. What remains are likely to be bound to defect/acidic Al sites in the support. This residual Cl appears to be persistently present in the catalyst, even after heating to 350 K under the flowing ethanol/water.

The subsequent effects Cl has on the evolution of the catalyst structures under the solvent flow are also varied. At 10 wt-% loading there is little difference between chlorinated and non-chlorinated samples. Only a difference in the average size of the final nanoparticles is implied, with the chlorinated system producing slightly smaller Pd nanoparticles. In this case, it is the intrinsic reactivity of the PdO phase that dominates the development of the catalysts.

At 5 wt-% loading a similar story is found, save for the fact that the presence of Cl causes a slight, but measurable, promotion (compared to the equivalent Cl-free Pd catalyst) of the reduction of the PdO phase. This is the case even though the Cl K-edge XANES shows that the majority of direct Cl–Pd^{II} bonding has been lost to the mobile solvent phase at ambient temperature.

In sharp contrast, the behaviour for the 1 wt-% Pd system is radically different. With its native form containing a high level of Cl, the Pd in this sample is found to be highly susceptible to reduction by the ethanol/water flow; wetting of this sample at room temperature causes the removal of the substantive Pd^{II}–Cl bonding, revealing the presence of a nascent Pd⁰ phase.

Subsequent spatial- and temporal-resolved Pd K-edge QEXAFS shows in more detail that the metal in 1 wt-% Pd/ γ - Al_2O_3 is reduced below 350 K. The contrast with the behaviour of the equivalent Cl-free catalyst is stark: the equivalent Cl-free catalyst is incredibly resistant to reduction, maintaining the PdO phase even after prolonged exposure to the flowing solvent

at 350 K, with a pronounced axial gradient of different Pd phases. In comparison, the facile reduction of the PdCl_2O_2 phase present in the chlorinated 1 wt-% Pd/ γ - Al_2O_3 catalyst resulted in a far more uniform axial profile.

In all cases, irrespective of the nature of the Pd precursor used, and in common with their Cl-free counterparts, the reduced Pd nanoparticles are found to be significantly contaminated by interstitial hydrogen, which appears to be intrinsic to the chemistry between the Pd and the solvent components [10–12].

In our previous work, we demonstrated that facile rearrangement of Pd nanoparticles can occur at ambient temperatures, under conditions that are commonly adopted for the preparation of catalyst material for microscopy: the use of alcohols to disperse the catalysts on the TEM grid, and consequently the bombardment of electrons, is enough for the solvent molecules to cause the Pd to rearrange, such that by the time a TEM micrograph is measured, the Pd is found to be in a nanoparticulate with average particle size of 2–4 nm, irrespective of loading or the support material [12]. This also appears to apply here for the 1 wt-% Pd sample that has a native PdCl_2O_2 oxychloride structure (determined by EXAFS): TEM imaging showed only the presence of Pd nanoparticles of average dimensions of *ca.* 3 nm.

The results obtained in this study can also be compared with that derived from encapsulated (ENCAT™ NP30) catalysts [13] where a variation in behaviour was also observed as a result of significant Cl contamination that arises from the use of chlorinated solvents in the encapsulation of the starting Pd(acetate) precursors. In this case we showed that, in batches of ENCAT™ NP30 where Cl was found to persist to a significant degree, that the reduction Pd is significantly curtailed rather than promoted.

These diverse observations lead us to conclude that the effects that Cl may have on the development of such catalysts in flowing solvents is not only dependent on the Pd phase initially present, but also the nature of the support material. Where Pd is present as predominantly nanosize PdO, Cl may be found to bond to defect sites within or upon the PdO particles. The direct bonding between Pd and Cl is weak and can be easily removed by an ethanolic solvent at ambient temperatures. However, a small persistent amount of Cl remains (Cl K-edge XANES), which is still bound to the Pd. Given the differences in ionic radii observed between Cl[−] (1.64 Å) and O^{2−} (1.24–1.28 Å) we might expect that any Cl still bound to a Pd centre within a largely PdO environment may induce a destabilising strain, that may promote the reductive collapse of the PdO phase. Evidence for this may be found in the case of the 5 wt-% Pd, where the onset of reduction is shifted to lower temperature in the chlorinated case than in the non-chlorinated, although the effect is small and completely absent when the Pd loading is increased to 10 wt-%.

On the other hand, when Cl is retained to such a degree (as in the 1wt-% Pd case) that a new oxychloride structure becomes tenable, the subsequent effects on reducibility in the solvents are much more profound; Pd nanoparticles may start to be formed and grow even at room temperature. In this case the solvent quickly removes Pd–Cl bonding, and the resulting unstable structure starts to form nanoparticles rather than being converted into the much more stable PdO.

More importantly it seems that in the case of the alumina the Cl is largely carried away with the solvent flow and therefore does not subsequently interfere with the evolution of the Pd nanoparticles. Where Pd is present as partially reduced entities and/or Pd(acetate) that are physically encapsulated in an organic (polyurea) matrix, the presence of Cl has the reversed effect, in that the reduction of the Pd to form reduced nanoparticles is highly suppressed. This could be due to the Cl binding to the nascent Pd particles, blocking further subsequent reduction as the Cl retained within the encapsulating polymer vesicles is largely prevented from being removed by the solvent, or that Cl may be held more tightly within the organic matrix, for example, through hydrogen bonding between the halide anion and the urea functionality. This also imply that physical encapsulation can be a more effective strategy to prevent the large scale reordering and transport of the very small reduced nanoparticles to form larger particles that was observed in catalysts supported on metal oxide surfaces.

Conclusions

Through the use of *in situ* QXAFS methods to address Pd and the K and L₃ edges and Cl at the K-edge we have delineated the effects that Cl may have on the development of Al₂O₃ supported Pd catalysts in contact with aqueous ethanolic solvent flows.

The degree to which Cl is retained and the degree to which it affects the development of reduced and nanoparticulate Pd is found to be a significant function of Pd loading and, specifically, in the limit of low (1 wt-%) loadings. In this limit Pd derived from PdCl₂ adopts a non PdO structure wherein high levels of Pd–Cl coordination are retained within structure of an approximate PdCl₂O₂ stoichiometry. This structure is far more susceptible to reduction by flowing ethanol/water than the nanosize stable PdO produced by the same synthetic approach at 5 and 10 wt-% Pd loadings, even though both Cl K-edge and Pd K-edge EXAFS show that the solvent mix removes the majority of Pd that is directly in contact with oxidised Pd centres. As such in the limit of low Pd loading the major effect of Cl is to significantly promote the formation of reduced Pd nanoparticles as compared to where Cl has not been present in the initial catalyst formulation: a result that is the exact opposite of that found when considering nanoparticle development in polymer encapsulated (ENCAT™ NP30) catalysts [13].

At higher loadings of Pd this promotional effect is progressively diminished such that at 10 wt-% loading Pd is reduced by the solvent in a manner equivalent to that observed in a Cl-free Pd catalyst or the same net Pd loading. At an intermediate (5 wt-%) loading evidence that Cl can also destabilise PdO to a degree toward reduction by the solvent flow is also forthcoming. In common with all the Pd catalysts we have recently studied in these manners, the resultant Pd nanoparticles are all suggested to be significantly contaminated by interstitial hydrogen sequestered from the solvent mixture.

As such we have shown that the effect Cl may have on the development of a Pd catalyst under such solvent mixtures is a strong function of Pd loading, the precise nature of the Pd present (PdO, PdCl₂O₂, or very small partially reduced Pd species) in the starting catalyst, and whether the Cl can be easily removed (or not) from the catalyst by the solvent flow.

Lastly, as in two other specific cases [12] we have also shown that when a native, non PdO, Pd phase is particularly reducible in face of an alcoholic solvent a significant disparity between how EXAFS and TEM report the structures of these catalysts emerges. This is a result of the ability of solvents commonly employed to disperse samples on to TEM grid to radically alter certain reducible forms of Pd (PdCl₂O₂ and very small 6–10 atom Pd clusters [12]) to facilitate initiate agglomeration of the Pd into nanoparticles of between 2 and 5 nm in diameter.

Acknowledgements

The Diamond light source are acknowledged for access to B18. We thank Johnson Matthey plc for the provision of Pd salts and catalysts. Ekaterina Wade (Imperial College) is acknowledged for assistance with the TEM measurements. MAN is very grateful to the University of Warwick (Physics) for a visiting academic position. RN thanks the University of Leeds for her scholarship.

Disclosure statement

No potential conflict of interest was reported by the authors.

Funding

This work was funded by EPSRC (UK), [grant number EP/G070172/1], [grant number EP/L003279/1] with additional contributions from the Pharmocat Consortium (AstraZeneca, GlaxoSmithKline and Pfizer). EMB was supported by Xunta Galicia, CJM by an EPSRC industrial Doctoral Training Grant (AstraZeneca).

ORCID

John B. Brazier  <http://orcid.org/0000-0001-5471-3469>

Stephen Parry  <http://orcid.org/0000-0001-5205-4543>

Christopher J. Mulligan  <http://orcid.org/0000-0003-1160-2202>

Klaus Hellgardt  <http://orcid.org/0000-0002-4630-1015>

King Kuok (Mimi) Hii  <http://orcid.org/0000-0002-1163-0505>

References

- [1]. Prat D, Hayler J, Wells A. A survey of solvent selection guides. *Green Chem.* **2014**;16:4546–4551.
- [2]. Prat D, Wells A, Hayler J, et al. CHEM21 selection guide of classical- and less classical-solvents. *Green Chem.* **2016**;18:288–296.
- [3]. Eastman HE, Jamieson C, Watson AJB. Development of solvent selection guides. *Aldrichim Acta.* **2015**;48:51–55.
- [4]. Henderson RK, Jiménez-González C, Constable DJC, et al. Expanding GSK's solvent selection guide – embedding sustainability into solvent selection starting at medicinal chemistry. *Green Chem.* **2011**;13:854–862.
- [5]. Negishi E-I, editor. *Handbook of organopalladium chemistry for organic synthesis*. New York (NY): Wiley; **2002**.
- [6]. Greco R, Goessler W, Cantillo D, et al. Benchmarking immobilized di- and triarylphosphine palladium catalysts for continuous-flow cross-coupling reactions: efficiency, durability, and metal leaching studies. *ACS Catal.* **2015**;5:1303–1312.
- [7]. Cantillo D, Kappe CO. Immobilized transition metals as catalysts for cross-couplings in continuous flow – a critical assessment of the reaction mechanism and metal leaching. *Chem Catal Chem.* **2014**;6:3286–3305.
- [8]. Mirza A, Hellgardt K, Williams MJ, et al. Factors affecting the leaching of palladium based homogeneous catalysts from controlled pore glass supports. *Conference Proceedings, 1997 Jubilee Research Event, Vols 1 and 2.* **1997**;1:1217–1220.
- [9]. Hii KK, Hellgardt K. Catalysis in flow: why leaching matters. *Top Organomet Chem.* **2015**;57:249–262.
- [10]. Brazier JB, Nguyen BN, Adrio LA, et al. Catalysis in flow: operando study of Pd catalyst speciation and leaching. *Catal Today.* **2014**;229:95–103.
- [11]. Newton MA, Brazier JB, Barreiro EM, et al. Operando XAFS of supported Pd nanoparticles in flowing ethanol/water mixtures: implications for catalysis. *Green Chem.* **2016**;18:406–411.
- [12]. Newton MA, Brazier JB, Barreiro EM, et al. Restructuring of supported Pd by green solvents: an operando quick EXAFS (QEXAFS) study and implications for the derivation of structure–function relationships in Pd catalysis. *Catal Sci Tech.* **2016**;6:8525–8531.
- [13]. Newton MA, Nicholls R, Brazier JB, et al. *Chem Commun.* Forthcoming.
- [14]. Kozlov SM, Aleksandrov HA, Neyman KM. Adsorbed and subsurface absorbed hydrogen atoms on bare and MgO(1 0 0)-supported Pd and Pt nanoparticles. *J Phys Chem C.* **2014**;118:15242–15250.
- [15]. Duś R. Reactivity of ethylene with selected forms of hydrogen deposit on evaporated palladium films. *Surf Sci.* **1975**;50:241–252.
- [16]. Teschner D, Borsodi J, Woosch A, et al. The roles of subsurface carbon and hydrogen in palladium-catalyzed alkyne hydrogenation. *Science.* **2008**;320:86–89.
- [17]. Nakamura S, Yasui T. The mechanism of the Palladium-catalyzed synthesis of vinyl acetate from ethylene in a heterogeneous gas reaction. *J Catal.* **1970**;17:366–374.
- [18]. Juszczak W, Łomot D, Karpiński Z, et al. Neopentane conversion over Pd/ γ -Al₂O₃. *Catal Lett.* **1995**;31:37–45.
- [19]. Lomot D, Juszczak W, Pielaszek J, et al. Structure and reactivity of supported Palladium catalysts. 1. Pd/SiO₂ prepared from PdCl₂. *New J Chem.* **1995**;19:263–273.
- [20]. Kappers M, Dossi C, Psaro R, et al. DRIFT study of CO chemisorption on organometallics-derived Pd/MgO catalysts: the effect of chlorine. *Catal Lett.* **1996**;39:183–189.
- [21]. Gaspar AB, Dieguez LC. Dispersion stability and methylcyclopentane hydrogenolysis in Pd/Al₂O₃ catalysts. *Appl Catal A.* **2000**;201:241–251.
- [22]. Le Normand F, Barrault J, Breault R, et al. Catalysis with palladium deposited on rare earth oxides – influence of the support on reforming and syngas activity and selectivity. *J Phys Chem.* **1991**;95:257–269.
- [23]. Soomro SS, Ansari FL, Chatziapostolou K, et al. Palladium leaching dependent on reaction parameters in Suzuki-Miyaura coupling reactions catalyzed by palladium supported on alumina under mild reaction conditions. *J Catal.* **2010**;273:138–146.
- [24]. Bonivardi AL, Baltanas MA. Preparation of Pd/SiO₂ catalysts for methanol synthesis. 3. Exposed metal fraction and hydrogen solubility. *J Catal.* **1992**;138:500–517.
- [25]. Dent AJ, Cibir G, Ramos S, et al. Performance of B18, the core EXAFS bending magnet beamline at diamond. *JPCS.* **2013**;430:012023.
- [26]. Dent AJ, Cibir G, Ramos S, et al. B18: a core XAS spectroscopy beamline for diamond. In DiCicco A, Filippini A, editors. *Conference Proceedings 14th International Conference on X-ray Absorption Fine Structure Journal of Physics: Conference Series, Vol. 190*; **2009**.
- [27]. Figueroa SJA, Prestipino C. A code devoted to handling large data sets. *JPCS.* **2016**;712:012012.
- [28]. Binsted N. PAXAS: programme for the analysis of X-ray adsorption spectra. University of Southampton; **1988**.
- [29]. Binsted N. EXCURV98 CCLRC Daresbury Laboratory computer program; **1998**.
- [30]. Thompson PBJ, Nguyen BN, Nicholls R, et al. X-ray spectroscopy for chemistry in the 2–4 keV energy regime at the XMaS beamline: ionic liquids, Rh and Pd catalysts in gas and liquid environments, and Cl contamination in γ -Al₂O₃. *J Synchrotron Radiat.* **2015**;22:1426–1439.
- [31]. Glaser T, Hedman B, Hodgson KO, et al. Ligand K-edge X-ray absorption spectroscopy: a direct probe of ligand–metal covalency. *Acc Chem Res.* **2000**;33:859–868.
- [32]. Shadle SE, Hedman B, Hodgson KO, et al. Ligand K-Edge X-ray-absorption spectroscopic studies – metal–ligand covalency in a series of transition metal tetrachlorides. *J Am Chem Soc.* **1995**;117:2259–2272.
- [33]. Sugiura C, Kitamura M, Muramatsu S. X-ray absorption near-edge structure of complex compounds (NH₄)₃RhCl₆, K₃RuCl₆, and Ru(NH₃)₆Cl₃. *J Chem Phys.* **1986**;84:4824–4827.
- [34]. Benfield RE. Mean coordination numbers and the non-metal–metal transition in clusters. *J Chem Soc Faraday Trans.* **1992**;88:1107–1110.
- [35]. Jentys A. Estimation of mean size and shape of small metal particles by EXAFS. *Phys Chem Chem Phys.* **1999**;1:4059–4063.